PROCESSING OF ORGANIC/INORGANIC COMPOSITES BY STEREOLITHOGRAPHY

J. H. LEE, R. K. PRUD'HOMME, and I. A. AKSAY
Department of Chemical Engineering and Princeton Materials Institute
Princeton University, Princeton, NJ 08544

ABSTRACT

Ceramic StereoLithography (CSL) is used to fabricate complex shaped ceramic powder compacts by laser photocuring a concentrated ceramic dispersion in photocuring solutions layer-by-layer. The main processing parameters in CSL such as layer thickness, resolution, hatch spacing, and overcure depend on knowledge of the light propagation in a concentrated dispersion. In studies dealing with the processing of ceramic-filled organics, we investigated the depth of curing for model resin systems as a function of photoinitiator concentration. An optimal photoinitiator concentration that maximized the gel cure depth was observed. The study showed that photoinitiator plays a significant role in controlling the quality and performance of the formed gel network, with special regard to thickness of cured layers. This has potential application to fields as diverse as industrially cured coatings and dental fillings, and more generally, 3-dimensional fabrication techniques.

INTRODUCTION

Stereolithography is a sequential layering process that converts a "virtual" object into a real structure [1,2]. A 3-dimensional, computer-aided design (CAD) model is computationally sliced into a series of 2-dimensional, thin patterns. Each 2-D pattern is then transmitted to another computer which controls a scanning laser [1,2]. The laser is rastered across the surface of a photocurable monomer resin to solidify the layer in the shape of the 2-D pattern. A new layer of resin is swept across the surface, and the process repeated. By sequentially depositing layers in this layer-additive fashion, the entire structure is replicated in solid form [1,2].

By their very nature, composite materials encompass a wide range of applications. Since stereolithography lends itself especially well to the fabrication of complex shaped objects, we narrow our focus to the processing of organic/inorganic hybrids for use as biomaterials. A specific goal is to produce bone graft or implant materials with complex internal geometry tailor-designed by computer. We desire to produce composites that are biocompatible from an immunological point of view, as well as mechanically functional in supporting loads. Current bone graft techniques suffer from a series of drawbacks [3]. Autogenous strategies are limited by finite supply and issues of morbidity. Allografts often involve issues of immunogenicity (potential for viral transmission) as well as efficacy, depending on sterilization method [3]. Commercial products such as ultra high molecular weight polyethylene lack bone inductivity and/or strength [4].

In processing of organic/inorganic composites by stereolithography, we have taken a two-pronged approach. We have previously developed techniques to produce fully ceramic compacts [5], and since the stereolithography apparatus (SLA) is designed for

pure polymeric constructs, we now marry both approaches to achieve the fabrication of ceramic/polymer hybrids. In developing these composites, we have found it necessary to develop monomer resins not available commercially. Furthermore, in optimizing these systems, we are currently studying the effect of photoinitiator concentration on curing depth.

MATERIALS AND METHODS

Organic/inorganic composites comprised of submicron size alumina (Al_2O_3) powder[a] as the inorganic phase (15% by volume) and a multi-functional monomer, *2,2-bis(4-(2-hydroxy-3-methacryloxypropoxy)phenyl) propane* (Bis-GMA)[b] as the organic matrix. We have fabricated the parts with an SLA[c]. Bis-GMA is a commonly employed monomer in the dental industry, and alumina is used by virtue of its extensive history as a biocompatible material [3]. The photoinitiator used was *2-benzyl-2-N,N-dimethylamino-1-(4-morpholinophenyl)-1-butanone* (DBMP)[d] (Fig. 1).

Because Bis-GMA has a viscosity of approximately 1200 Pa·s, trichloroethylene (TCE) was used as a diluent solvent for the monomer in a 40/60 weight ratio. Resin was pipetted into cylindrical wells and filled to the brim. A glass coverslide placed in contact with the top of the solution acted as a substrate for attachment during the polymerization. Samples were cured by writing a cross-hatched pattern with dimensions shown in Fig. 2(a). Solid composites were formed at energy dosages of 1.702 J/cm^2 and 22.255 J/cm^2.
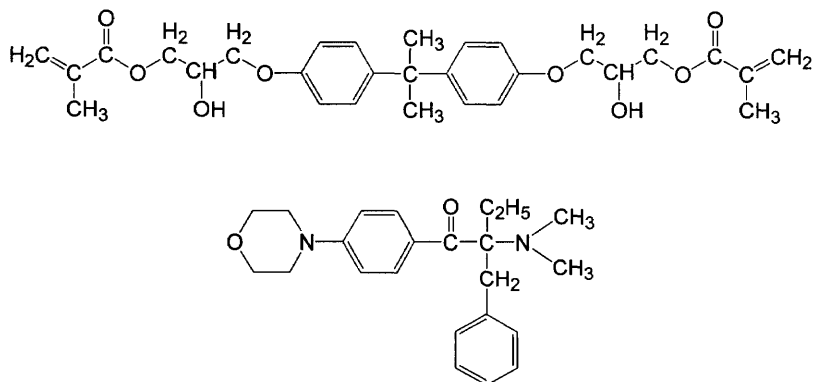

Figure 1: Chemical structures for *2,2-bis(4-(2-hydroxy-3-methacryloxypropoxy)phenyl) propane (Bis-GMA)* and *2-benzyl-2-N,N-dimethylamino-1-(4-morpholinophenyl)-1-butanone* (DBMP).
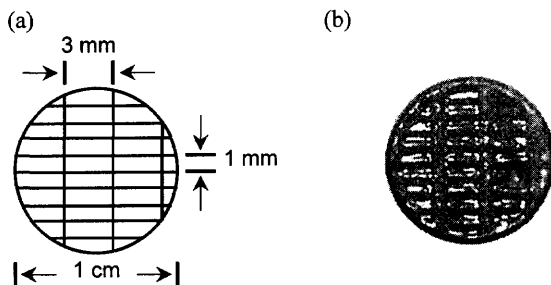
Figure 2: (a) CAD schematic of UV-cured disc. Black lines represent cross-hatched laser rastering pattern (laser beam diameter of 250 μm and wavelength of 325 nm); (b) Bis-GMA/alumina (10/90 by volume) thin film composite formed in the SLA. Note that the designed architecture of the CAD file has been reproduced successfully.

In the fabricated composites, the CAD cross-hatched pattern was replicated successfully (Fig. 2(b)). Use of the glass coverslide facilitated removal of the gel for thickness measurements. Because of operating constraints with the SLA, individual layer thicknesses should have an order of magnitude of 100 μm to achieve successful layer lamination and adhesion. As clarified in earlier work, the introduction of ceramic filler particles into the photocurable resin results in scattering effects, which effectively decrease the mean transport length of photons through the resin [6,7]. Thus, it is desirable to maximize the curing depth in the homopolymer resin before the addition of ceramic to ensure suitable cure depths are obtained in the composite material.

The "standard design equation" for stereolithography presented by Jacobs provides a relationship between cure depth and energy dosage as follows [1,2]:

$$C_d = D_p ln\left(\frac{E_{max}}{E_c}\right),\tag{1}$$

where C_d is the cure depth, D_p is the depth of penetration of the laser beam into the solution, E_{max} is the energy dosage per area, and E_c represents the critical energy dosage. This empirical equation is used to fit experimental data on cure depth versus energy dose (E_{max}) to determine values for D_p and the empirical constant E_c. These values are then used to determine layer thicknesses of each layer for stereolithographic fabrication. Thus, one way to increase cure depth is to increase energy dosage. Noting, however, that the energy dosages employed in fabrication of the Bis-GMA/alumina composites described above are higher than those typically required for the commercially available resins the SLA was designed for, another method of increasing cure depth is desired. Therefore, the effect of photoinitiator concentration on cure depth was probed to this end.

Solutions of Bis-GMA and TCE were again prepared in the manner described above. Photoinitiator (PI) concentration was varied from 0.3×10^{-3} to 5.1×10^{-3} moles/liter, corresponding to 0.010 to 0.150 weight percent of total solution and 0.0167 to 0.2500 weight

percent based on Bis-GMA monomer weight. These values are comparable to typical industrial formulations. Samples were cured at 3 dosage levels: 0.931, 1.702, and 22.255 J/cm^2. Dosages were varied by varying the laser beam writing speed on the SLA. Cure depth was then measured using a micrometer.

RESULTS AND DISCUSSION

The experimental results are shown in Fig. 3 for the patterned photopolymerized films. The ordinate is the gel thickness in millimeters and the abscissa the photoinitiator concentration from 0.3 to 5.1 mM, which corresponds to 0.017 to 0.250 weight percent based on Bis-GMA monomer weight. The corresponding weight percent photoinitiator (0.01 to 0.15) based on total weight of solution is shown above. The three data curves correspond to three different laser energy dosages.
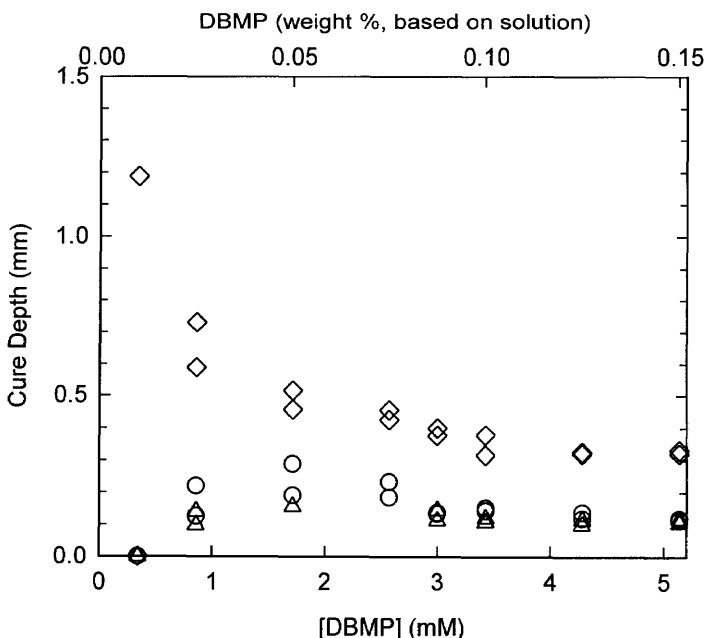

Figure 3: Gel thickness versus photoinitiator concentration. The three data curves correspond to the three different laser energy dosages (◇ 22.255 J/cm^2, ○ 1.702 J/cm^2, and △ 0.931 J/cm^2). Photoinitiator concentration is given in millimoles/liter on the bottom abscissa, and as weight percent based on total solution on the top abscissa. Note the existence of an optimal photoinitiator concentration that maximizes cure depth.

It might be expected that cure depth should increase with increasing photoinitiator concentration [8-10]; however, this is not the case. The experimental data show that an optimal photoinitiator exists for which cure depth is maximized. Furthermore, this dependence is not adequately explained by the standard design equation for stereolitho-

graphy, which only directly considers the effect of energy dosage on cure depth. Extended data points (not shown) were taken for higher photoinitiator concentrations to confirm that the curve continues to decrease monotonically.

Returning to the filled resin, the degree of attenuation of the laser beam into the colloidal suspension medium is exacerbated by a multiple scattering effect. As filler is introduced into the system, the mean transport path of photons into the solution decreases, thereby altering the curing properties of the resin [6,7]. With the assumption that interference effects in the medium (modeled here as semi-infinite) can be neglected, a complete description of photon transport can be made in terms of the number of photons per unit volume per unit direction. In this diffusion model for scattering, two length scales characteristic of the medium, are important in describing the photon density in the medium [6]. The absorption length, l_a, represents the average distance traveled by the photon before being absorbed. For purely absorbing resin this represents the penetration depth. The transport mean free path-length, l_{tr}, is the average distance the photon travels before its propagation direction is completely randomized. Using a Percus-Yevick structure factor, $S(\theta)$, for hard sphere scatterers, l_{tr} may be calculated as [6]:

$$l_{tr} = \left(n\sigma_{tr}\right)^{-1},$$ (2)

where n is the number density of scatterers and σ_{tr} is the transport scattering cross-section of a single scatterer, found as:

$$\sigma_{tr} = \int \frac{d\sigma}{d\Omega}\left(1 - \cos(\theta)\right)S(\theta)d\Omega,$$ (3)

where $d\sigma/d\Omega$ is the differential scattering cross-section scaled by $(1-\cos(\theta))$ to account for anisotropic scattering. This in turn allows the calculation of the actinic intensity profile as a function of l_a. Solution of the diffusion equation gives expressions that allow for the rescaling of the absorption length in medium without particles, l_m, based on volume fraction filler, ϕ, as:

$$\frac{1}{l_a} = \left(\frac{\phi}{\phi_m}\right)^{1/3}\left(\frac{\phi_m^{1/3} - \phi^{1/3}}{\phi^{1/3}l_m} + \frac{1}{l_p}\right),$$ (4)

where ϕ_m is the maximum packing fraction for the colloidal dispersion and l_p is defined as the length scale where the light intensity decays by a factor e^{-1} traveling through the particle. Support for this determination of the absorption length for photon propagation through dense colloidal dispersion was provided by pulse-chase dye experiments to simulate the actinic absorption of the photocuring resin [6,7]. Figure 4 summarizes the results of the experiment [6]. As the data show, the transport length decreases dramatically with increasing filler volume fraction. Note that without correction for multiple scattering, the deviation between actual transport length and calculated value grows as

volume fraction rises. Thus, rescaling of the transport length by Eq. (4) is necessary in order to accurately predict the curing profile for ceramic resin.
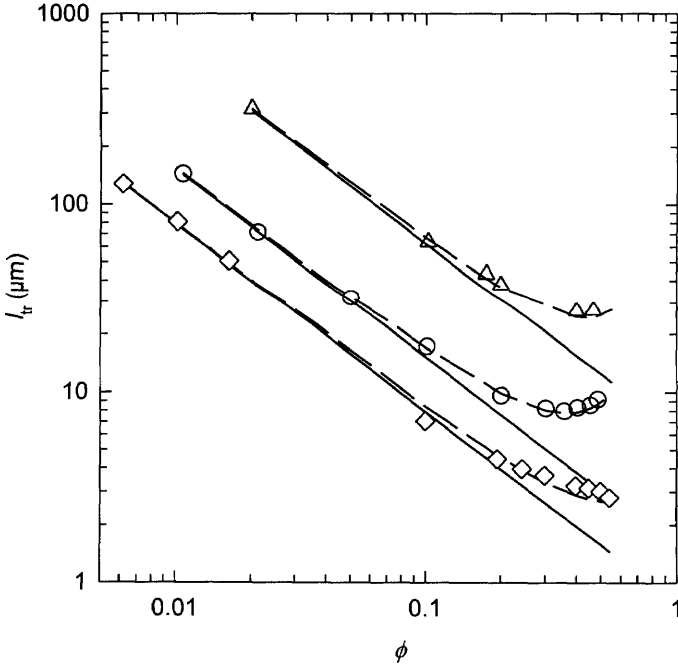

Figure 4: Transport mean free path versus volume fraction, ϕ, of scattering particles on log-log scale. Solid curves are computed values without correlation and σ_{tr}; dashed curves are computed values obtained by using equations (2)-(4) and $S(\theta)$ from Percus-Yevick theory. Symbols represent transport lengths obtained from experiment: ◇ 0.51 µm alumina, △ 0.46 µm silica, and ◯ 0.32 µm alumina, and. The curve for 0.51 µm alumina has been shifted up by log(3) for clarity. (reprinted by permission [6])

While the model described above elucidates the dependence of the curing profile on filler fraction, it does not suggest the shape of the cure depth versus photoinitiator concentration curve seen in Fig. 3. To address this second issue, we have explored this dependence through experimental work with the homopolymerization reaction of Bis-GMA. We have also developed a model from first principles to incorporate the photoinitiator dependence [11].

CONCLUSIONS

In this paper, we report the successful processing of Bis-GMA/alumina organic/inorganic biocomposites via stereolithography. Additionally, controlled patterning of the composite has been demonstrated through replication of designed architecture via CAD. In obtaining feasible cure depths to enable fabrication of multi-layered objects, we note the desire to increase cure depth by an alternative route than simply increasing energy dosage. A model for the role of volume fraction ceramic filler on the curing profile was developed and corroborated with experiment. We now demonstrate the dependence of the curing depth on photoinitiator concentration, and show the existence of an optimal photoinitiator concentration for which cure depth is maximized. Elsewhere [11], we quantitatively probe this dependence using a model derived from first principles to explain the experimental results. Once clarified, dependence of the cure depth on photoinitiator concentration should provide implications to fields as diverse as industrially cured coatings and dental fillings, in addition to our own particular interest in 3-dimensional fabrication techniques.

ACKNOWLEDGEMENTS

REFERENCES

1. P.F. Jacobs, *Rapid Prototyping & Manufacturing*, (Soc. of Manufacturing Engineers, Dearborn, MI 1992).

2. P.F. Jacobs, *Stereolithography and other RP&M Technologies* (Soc. of Manufacturing Engineers, Dearborn, MI 1996).

3. L.L. Hench, "Bioceramics," *J. Am. Ceram. Soc.* **81** [7] 1705-28 (1998).

4. W. Bonfield, M.D. Grynpas, A.E. Tully *et al.*, "Hydroxyapatite Reinforced Polyethylene - a Mechanically Compatible Implant Material For Bone-Replacement," *Biomaterials* **2** [3] 185-86 (1981).

5. R. Garg, "*Stereolithography of Ceramics*," Ph.D. dissertation (Princeton University, Princeton, NJ, 1999).

6. R. Garg, R.K. Prud'homme, I.A. Aksay, F. Liu, and R. Alfano, "Optical Transmission in Highly-Concentrated Dispersions," *J. Opt. Soc. Am.* **15** [4] 932-35 (1998).

7. R. Garg, R.K. Prud'homme, I.A. Aksay, F. Liu, and R. Alfano, "Absorption Length for Photon Propagation in Highly Dense Colloidal Dispersions," *J. Mater. Res.* **13** [12] 3463-67 (1998).

8. G.A. Brady and J.W. Halloran, "Differential Photo-calorimetry of Photopolymerizable Ceramic Suspensions," *J. Mater. Sci.* **33** [18] 4551-60 (1998).

9. F.A. Rueggeberg, P.E. Lockwood, and J.W. Ergle, "Effect of Post-cure Heating and Photoinitiator Level on a Model Resin System," *J. Dental Res.* **76** 472-72 (1997).

10. F.A. Rueggeberg, J.W. Ergle, and P.E. Lockwood, "Effect of Photoinitiator Level on Properties of a Light-cured and Post-cure Heated Model Resin System," *Dental Materials* **13** [5-6] 360-64 (1997).

11. J.H. Lee, R.K. Prud'homme, and I.A. Aksay, "Cure Depths in Photopolymerization: Theory and Experiments," *J. Mater. Res.* submitted (2000).